

The dynamics of cell cycle regulation

John J. Tyson,^{1*} Attila Csikasz-Nagy,^{2,3} and Bela Novak²

Summary

Major events of the cell cycle—DNA synthesis, mitosis and cell division—are regulated by a complex network of protein interactions that control the activities of cyclin-dependent kinases. The network can be modeled by a set of nonlinear differential equations and its behavior predicted by numerical simulation. Computer simulations are necessary for detailed quantitative comparisons between theory and experiment, but they give little insight into the qualitative dynamics of the control system and how molecular interactions determine the fundamental physiological properties of cell replication. To that end, bifurcation diagrams are a useful analytical tool, providing new views of the dynamical organization of the cell cycle, the role of checkpoints in assuring the integrity of the genome, and the abnormal regulation of cell cycle events in mutants. These claims are demonstrated by an analysis of cell cycle regulation in fission yeast. *BioEssays* 24:1095–1109, 2002.

© 2002 Wiley Periodicals, Inc.

Introduction

The fundamental goal of molecular cell biology is to understand how the information encoded in the cell's genome is used to direct the complex repertoire of physiological responses of the cell to its environment, in order to keep the cell alive and to propagate its genome to a new generation. At one end of this continuum, nucleotide sequences direct the synthesis of

polypeptide chains, which then fold into three-dimensional structures with basic functions as enzymes, motors, channels, cytoskeletal components, etc. At the other end, complex assemblages of interacting proteins carry out the fundamental chores of life: energy metabolism, biosynthesis, signal transduction, movement, differentiation, and reproduction. The triumph of molecular biology of the last half of the twentieth century was to identify and characterize the molecular components of this machine, epitomized by the complete sequencing of the human genome. The grand challenge of post-genomic cell biology is to assemble these pieces into a working model of a living, responding, reproducing cell; a model that gives a reliable account of how the physiological properties of a cell derive from its underlying molecular machinery.

If one thinks of the genome as the “parts list” of a cell, then this model of interacting proteins is essentially the “users’ guide,” telling not only how a cell works but also how one might fix it when it’s broken or re-engineer it to different specifications. Although the life sciences community is many years away from this goal, it is now recognized as a worthy and ultimately achievable pursuit. However, to reach this goal will require new ways of doing molecular biology: experimental approaches that are more holistic and synthetic than reductionistic, and theoretical approaches that respect the complexity of the molecular machinery of life.

In 1999 Hartwell, Hopfield, Leibler & Murray called for a new theoretical approach to molecular cell biology in these words⁽¹⁾: “The best test of our understanding of cells will be to make quantitative predictions about their behavior and test them. This will require detailed simulations of the biochemical processes taking place within [cells]... [In addition, we] need to develop simplifying, higher-level models and find general principles that will allow us to grasp and manipulate the functions of [biochemical networks].” These authors are saying that a useful theory must (1) provide realistic, accurate, predictive simulations of complex biochemical networks and (2) reveal the general principles by which proteins control the adaptive behavior of cells. In a series of publications starting in 1993, we have been trying to provide this two-fold view of the molecular basis of eukaryotic cell cycle regulation.^(2–7) In this review, we summarize the conclusions of ten years of research, putting special emphasis on bifurcation theory as a tool for revealing the general principles of cell cycle control.

¹Department of Biology, Virginia Polytechnic Institute & State University, USA.

²Department of Agricultural Chemical Technology, Budapest University of Technology and Economics, Hungary.

³Bekesy Postdoctoral Fellow.

Funding agency: NSF; Grant number: MCB-0078920. Funding agency: DARPA/AFRL; Grant number: F30602-02-0572. Funding agency: James S. McDonnell Foundation; Grant number: 21002050. Funding agency: OTKA; Grant number: T-032015.

*Correspondence to: John Tyson, Department of Biology, Virginia Polytechnic Institute & State University, Blacksburg VA 24061, USA. E-mail: tyson@vt.edu

DOI 10.1002/bies.10191

Published online in Wiley InterScience (www.interscience.wiley.com).

Abbreviations: CDK, cyclin-dependent kinase; APC, anaphase-promoting complex

Cell cycle regulation

Physiology

The cell cycle is the process by which one cell becomes two. Conceptually, we can distinguish between the chromosome cycle (DNA replication, followed by physical separation of the two complete genomes to daughter nuclei) and the growth cycle (replication of all other components of a cell—proteins, membranes, organelles, etc.—and their physical separation to daughter cells). It is essential that the genome be accurately replicated and carefully partitioned to daughter nuclei, so that each new cell contains all the information necessary to perpetuate the cell type. The growth cycle can be a little sloppier; the newborn cell needs a certain minimum complement of structures and machinery to survive, but short-changes at division can be compensated by macromolecular synthesis directed by the genome. Nonetheless, it is essential that the chromosome and growth cycles be coordinated in the long run, so that cells replicate their DNA and divide each time they grow by a factor of two. Were this not so, cells would get progressively larger or smaller each generation, both with fatal consequences.

In eukaryotic cells, the chromosome cycle (Fig. 1) consists of two basic processes: DNA synthesis (S phase) and mitosis (M phase). During S phase, double-stranded DNA molecules are replicated to produce pairs of “sister chromatids” held together by proteins called cohesins.⁽⁸⁾ M phase consists of four subphases: prophase (when replicated chromo-

somes condense into compact structures), metaphase (when condensed chromosomes are aligned on the midplane of the mitotic spindle), anaphase (when cohesins are degraded and sister chromatids are partitioned into two separate bundles), and telophase (when daughter nuclei form and the cell begins to divide). S and M phases are separated in time by two “gap” (G_1 and G_2 phases), constituting the generic cell cycle: G_1 –S– G_2 –M.

It is crucial that S and M phases alternate in time. If a haploid cell attempts two mitotic nuclear divisions in a row, without a complete intervening S phase, its progeny will inherit grossly incomplete genomes and die. Repeated S phases without intervening mitoses, is not immediately fatal (it produces large, polyploid cells), but it is unusual (occurring naturally in ciliates and in some terminally differentiated cells).

Proper progression through the cell cycle—alternation of S and M phases, and coordination of growth and division—is assured by “checkpoints” that guard crucial transitions in the chromosome cycle (see Fig. 1). The G_1 checkpoint controls entry into S phase, making sure that (1) cells are large enough to warrant a new round of DNA synthesis, (2) any damage suffered by the DNA has been repaired, and (3) external conditions are favorable for mitotic cell division.⁽⁹⁾ For yeast cells, favorable external conditions are the presence of certain nutrients in the surroundings and the absence of sex pheromones that initiate conjugation and meiotic division. Mitotic reproduction in multicellular organisms is under much more complex, external regulation, mediated by growth hormones,

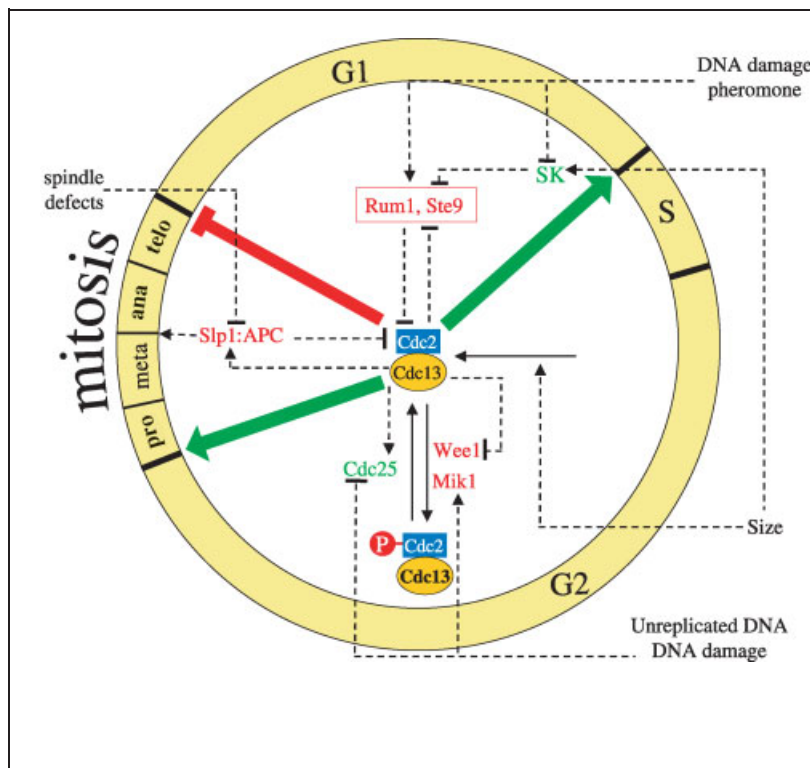


Figure 1. The cell cycle engine in fission yeast. The eukaryotic cell cycle is divided into four phases: G_1 , S (DNA synthesis), G_2 , and M (prophase, metaphase, anaphase, telophase). The G_1 -to-S and G_2 -to-M transitions are driven by rising activity of a protein kinase, Cdc2:Cdc13. Exit from mitosis (anaphase and telophase) is inhibited by high activity of Cdc2:Cdc13 and promoted by activation of Slp1:APC, which destroys Cdc13. Cdc2:Cdc13 is kept low during G_1 by the actions of Rum1 and Ste9. Starter kinases (SK) help Cdc2:Cdc13 to make a comeback at the end of G_1 . During S and G_2 , Cdc2:Cdc13 is kept in a less active, phosphorylated form by Wee1 and Mik1. Cdc25 removes the inhibitory phosphate, as the cell enters M phase. Progress from one phase to the next is promoted by growth and can be blocked or delayed at checkpoints, where surveillance mechanisms exercise quality controls over DNA replication, DNA repair, and mitotic spindle assembly. (Adapted from Novak B, Sible JC, Tyson JJ. Checkpoints in the cell cycle. In: Encyclopedia of Life Sciences, Macmillan Reference Ltd., 2002.)

cell–cell contacts, and other constraints necessary for multicellularity.

The G₂ checkpoint guards entry in mitosis, making sure that (1) DNA is fully replicated, (2) any new damage sustained by the DNA has been repaired, and (3) the cell is large enough to divide. The metaphase checkpoint guards the metaphase-to-anaphase transition.⁽¹⁰⁾ Chromosomes must be properly aligned on the mitotic spindle, with sister chromatids attached to opposite poles, before the cohesins are degraded. If problems arise in assembling the spindle or aligning the chromosomes, the metaphase checkpoint blocks activation of the mitotic exit network.

A morphogenetic checkpoint in budding yeast arrests cells in G₂ if a bud fails to form.⁽¹¹⁾ If fission yeast cells fail to septate, a cytokinesis checkpoint blocks them in the next G₂ phase.⁽¹²⁾ New checkpoints continue to be uncovered and characterized.

Molecular mechanism

Because the cell cycle plays a central role in all processes of biological growth, reproduction and development, cell biologists have invested much effort in identifying the molecular components and protein interactions underlying its control. The master molecules of the cell cycle are enzymes called cyclin-dependent protein kinases (CDKs). As their name implies, CDKs require a cyclin partner to be active. When associated with appropriate cyclins, CDKs trigger major events of the chromosome cycle (DNA replication, nuclear envelope breakdown, chromosome condensation, spindle assembly) by phosphorylating certain target proteins on chromosomes and elsewhere. The destruction of mitotic CDK activity at anaphase allows cells to divide and enter G₁ phase of the next cell cycle.⁽¹³⁾ Exit from mitosis is controlled by the anaphase-promoting complex (APC), which initiates the degradation of cohesins and mitotic cyclins.⁽¹⁴⁾ Hence, to understand the molecular control of cell reproduction is to understand the regulation of CDK and APC activities.^(14,15)

Cell cycle regulatory genes have been studied in great detail for a variety of organisms: budding yeast, fission yeast, *Aspergillus*, *Arabidopsis*, fruit fly eggs, frog eggs, and mammalian cells. Although there are significant differences in machinery from one cell type to another, the underlying “cell cycle engine” (CDK and APC regulation) is remarkably conserved. For the purposes of this review, we concentrate on the molecular interactions (see Fig. 1) underlying the mitotic cycle of fission yeast, *Schizosaccharomyces pombe*. In this organism, a single CDK (called Cdc2) in combination with a single B-type cyclin (called Cdc13) triggers both S phase (at modest Cdc2 activity) and M phase (at high Cdc2 activity).⁽¹⁵⁾ The activity of Cdc2:Cdc13 is regulated in three different ways (Fig. 1):

- Availability of cyclin subunits.
- Phosphorylation of kinase subunits.
- Binding to a stoichiometric inhibitor.

Although the intracellular concentration of Cdc2 does not vary throughout the cell cycle, the concentration of Cdc13 fluctuates considerably, being low in G₁ and rising steadily through S, G₂ and early M phases.⁽¹⁶⁾ Cdc13 level is low in G₁ because, although it is constitutively synthesized, it is rapidly degraded as cells exit mitosis and throughout G₁ phase.⁽¹⁷⁾ Cdc13 degradation is mediated by two proteins, Slp1 and Ste9, which target Cdc13 for ubiquitination by the APC and subsequent destruction by proteasomes.^(18–20) Furthermore, during G₁ phase, cells contain a protein, Rum1, which binds to and inhibits any Cdc2:Cdc13 dimers that may be present.^(21,22) To leave G₁ and enter S phase, Ste9 and Rum1 must be neutralized; this transition is aided by the accumulation of a set of starter kinases (Cdc2 in combination with “G₁ cyclins,” Cig1, Cig2 and Puc1), which are not opposed (or only weakly opposed) by Ste9 and Rum1.^(17,23) The starter kinases phosphorylate Ste9 and Rum1, thereby inactivating them and labeling them for degradation. During G₂ phase, when Cdc13 is relatively stable and Rum1 is absent, Cdc2:Cdc13 dimers are held in an inactive, tyrosine-phosphorylated form, PCdc2:Cdc13. The extent of Cdc2 phosphorylation is controlled by two kinases, Wee1 and Mik1,⁽²⁴⁾ and an opposing phosphatase, Cdc25.⁽²⁵⁾ To enter mitosis with high Cdc2 activity, Wee1 and Mik1 must be inactivated and Cdc25 activated. This transition is aided by cell growth to a critical size. Finally, to exit mitosis, Cdc2:Cdc13 activity must be destroyed, Ste9 activated, and Rum1 stockpiled. This transition is aided by Slp1:APC, which itself is indirectly activated by Cdc2:Cdc13. By causing substantial degradation of Cdc13, Slp1 allows Ste9 and Rum1 to reassert themselves.

The molecular regulatory system in mammalian cells is much more complex than that in yeast, but the core cell cycle engine is quite similar. Mammalian cells contain all the molecular components found in yeast, interacting in similar ways, but often as multigenic families encoding proteins of slightly different functions.⁽²⁶⁾ For example, mammals have multiple kinases (Cdk1, Cdk2, Cdk4, ...), multiple cyclins (A, B, D, E, ...), multiple CDK inhibitors (p16, p21, p27, ...), and multiple phosphatases (Cdc25A, B and C). It is much easier to understand the molecular basis of cell cycle control in fission yeast, and there is good reason to suspect that its generic properties carry over in part to the more complex controls over cell division in animals and plants.

Wild-type cells

Toggle switches, amplifiers and oscillators

To understand how the control system in Fig. 1 works, we need a little more information. The proteins that modulate Cdc2 activity are themselves modulated by Cdc2:Cdc13, through a set of feedback loops.⁽²⁷⁾

- Rum1 inhibits Cdc2:Cdc13, but Cdc2:Cdc13 phosphorylates Rum1, thereby targeting Rum1 for degradation.

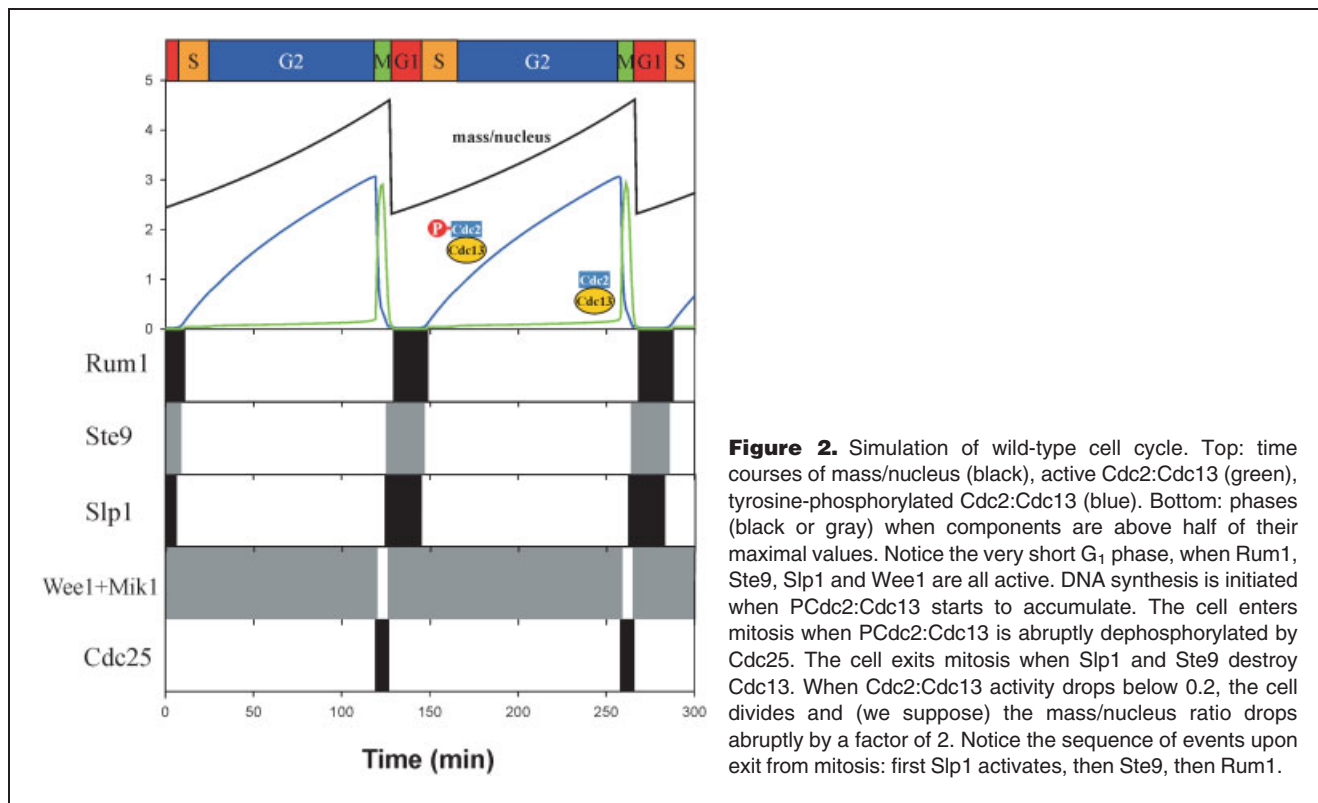
- Ste9:APC labels Cdc13 for degradation, but Cdc2:Cdc13 can phosphorylate Ste9, thereby downregulating its activity and targeting it for degradation.
- Wee1 phosphorylates and inactivates Cdc2:Cdc13, but, at the same time, Cdc2:Cdc13 is trying to phosphorylate and inactivate Wee1.
- Cdc25 takes the inactivating phosphate group off PCdc2:Cdc13, and Cdc2:Cdc13 returns the favor by phosphorylating and thereby activating Cdc25.
- Slp1:APC, which also labels Cdc13 for degradation, is itself activated by Cdc2:Cdc13 by an indirect pathway.

The first three feedback loops are examples of mutual antagonism. Under appropriate conditions, the antagonists cannot coexist, i.e. the feedback loop works like a toggle switch. Either Cdc2:Cdc13 has the upper hand and its antagonist (Rum1 or Ste9 or Wee1) is suppressed, or vice versa. The fourth interaction is a positive feedback loop: Cdc2 and Cdc25 activate each other in a mutually amplifying fashion. The last interaction is a time-delayed negative feedback loop, which, under appropriate conditions, can generate oscillations (as Cdc2:Cdc13 concentration rises, it turns on Slp1, which targets Cdc13 for degradation, causing Cdc2:Cdc13 concentration to fall, and Slp1 to turn off).

The state of these feedback loops responds to cell size. Small cells tend to be in G₁ phase (with little Cdc2 activity);

medium-sized cells tend to be in S–G₂ phase; large cells tend to be in M phase, with Cdc25 active and Wee1 inactive.^(28,29) It is this responsiveness of the Cdc2 control system to cell size that coordinates the chromosome cycle to cell growth. To model these effects, we assume that Cdc13 is synthesized at a rate proportional to cell mass (i.e., number of ribosomes), and then it combines with Cdc2 and moves into the nucleus, where its effective nuclear concentration increases steadily as the cell grows. Hence, an important determinant of the state of the Cdc2 control system is the mass/nucleus ratio.⁽²⁷⁾

To study the dynamical consequences of these feedback loops, one must formulate these interactions as a precise molecular mechanism, convert the mechanism into a set of nonlinear ordinary differential equations, and study the solutions of the differential equations by numerical simulation (Fig. 2). This procedure is explained in detail in earlier publications.⁽³⁰⁾ Although numerical simulations are crucial for quantitative comparisons of theory and experiment, the qualitative relationships between kinetic equations and cell physiology are most clearly revealed by the methods of dynamical systems theory (Box 1). We have recently summarized these basic theoretical ideas and their relevance to cell biology.⁽²⁷⁾ In this review, we pick up where we left off in that paper, using bifurcation diagrams to provide a new perspective on cell cycle checkpoints and mutant phenotypes in fission yeast.



BOX 1: PRIMER ON DYNAMICAL SYSTEMS

The relevance of dynamical systems theory to cell physiology is described in a number of review articles.^(7,27,47–49) Thorough presentations of the theory are available in many excellent textbooks.^(50–53)

For our purposes, a dynamical system is a set of nonlinear ordinary differential equations,

$$\frac{dx_i}{dt} = f_i(x_1, \dots, x_n; p_1, \dots, p_m), \quad i = 1, \dots, n$$

where x_i = concentration (or activity) of the i -th protein in the reaction network, and p_j = value of the j -th parameter (rate constant, binding constant, etc.). The functions f_i are all of the form f_i = synthesis – degradation + activation – inactivation, where “synthesis” etc. are nonlinear functions of the variable concentrations and constant parameters in the model. The exact forms of these functions depend on the stoichiometry of the reaction network and the assumptions made about the rate laws for each reaction. A model has three parts: a set of rate equations $\{f_1, \dots, f_n\}$, a set of parameter values $\{p_1, \dots, p_m\}$, and a set of initial conditions $\{x_1(0), \dots, x_n(0)\}$. Once these three sets are specified, the differential equations can be solved numerically to give the time-dependence of each component protein. In principle, these time courses, $x_i(t)$ for $0 \leq t \leq t_{\text{end}}$, determine all the physiological properties of the reaction network.

We are primarily interested in “steady state” and “oscillatory” solutions of the dynamical system. At a steady state $\{x_1^*, \dots, x_n^*\}$, the rates of change are all identically zero: $f_i(x_1^*, \dots, x_n^*, p_1, \dots, p_m) = 0$ for all i . Hence, at a steady state, protein concentrations are unchanging in time. For an oscillatory solution, protein concentrations change in time, repeating themselves after a characteristic period $T_{\text{osc}} > 0$.

Recurrent solutions (steady states or oscillations) can be either stable or unstable. A steady state is stable if any small perturbation away from the steady state disappears over time, and the control system returns to the steady state. The state is unstable if some perturbations grow larger with time, and the control system leaves the vicinity of the steady state. (For example, a damped pendulum comes to rest at a stable steady state with the bob hanging directly below the pivot point, but the pendulum also has an unstable steady state with the bob precariously balanced directly above the pivot point.) Stable solutions represent physiologically observable states of the control system; unstable solutions make their presence known only indirectly. (Gymnasts use the pendulum’s unstable

steady state to great advantage in their routines on the high bar.) Similar notions of stability and instability apply to oscillatory solutions.

The nature of the recurrent solutions of a dynamical system depends on the precise values of the parameters in the model. If a parameter value is changed (e.g., a molecular geneticist might change the rate of synthesis of a certain protein by introducing its gene on a plasmid under the control of an inducible promoter), then the properties of the recurrent solutions of the network may change. For example, a stable steady state may lose its stability or even cease to exist, and an oscillatory solution may pop into existence. Qualitative changes, such as these, in the nature of the recurrent solutions of a dynamical system are called “bifurcations”. They occur at specific values of the parameters, called “bifurcation points”.

The bifurcations of a dynamical system can be characterized by a one-parameter bifurcation diagram. To construct such a diagram, the investigator singles out one variable (say, x_1) as a representative of all the dynamic variables in the control system and one parameter (say, p_1) as a representative of all the rate-determining factors in the model. Scanning across the parameter value, the investigator plots the steady-state value x_1^* as a function of p_1 . At bifurcation points, strange things happen to this function.

Let’s illustrate these ideas with a specific example: the seesaw in the accompanying Fig. A. The dynamical variables of the system are the position and velocity of the ball along the beam, and the angle and angular velocity of the beam around the fulcrum. The parameters are things like the mass of the ball (m), the acceleration of gravity (g), the height of the pivot (h), the length of the beam ($2L$) and its moment of inertia (I), and the torque (τ) applied to the end of the seesaw. The differential equations governing this system can be derived from Newton’s second law of motion ($F = ma$) for the ball and the beam. They are quite complicated, because of the constraints on the ball’s motion due to the beam, and the beam’s motion due to the ground. We don’t need to write them down or analyze them mathematically, because we are all quite familiar with the behavior of this little toy. For any given values of the parameters, the ball quickly comes to rest at either the left or right stop, with the seesaw usually in contact with the ground. These are the two stable steady states of the dynamical system. Which steady state the system reaches depends on the parameter settings (especially the torque) and on the initial conditions of the ball (its initial

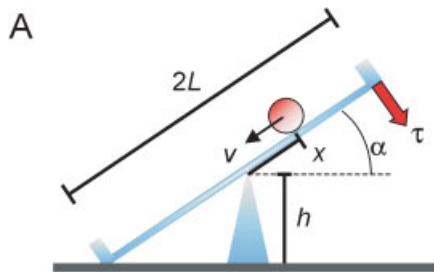


Figure A (Box 1). A seesaw. A ball of mass m rolls along a beam of length $2L$, pivoting on a fulcrum of height h . The state of the ball is characterized by its position on the beam (x) and its velocity (v). The state of the beam is given by its angle to the horizontal (α) and its angular velocity. The ball can come to rest at stops on the left and right ends of the beam. By applying torque (τ) at the right end of the beam, we can tip the seesaw between two stable steady states: left side down or right side down. This mechanical toggle switch bears many similarities to the biochemical toggle switches that underlie progression through the cell cycle.

position and velocity) and the beam (its initial angle and rotational velocity).

In Fig. B we plot the steady-state position of the ball as a function of the applied torque. This is a one-parameter bifurcation diagram. We use just one variable (position of the ball along the beam) to indicate the state of the system, and we single out one parameter (torque) to explore. (We hold m , h , L and g fixed; there's not much we can do about g .) Positive torque is a clockwise force applied to the right stop, and negative torque is a

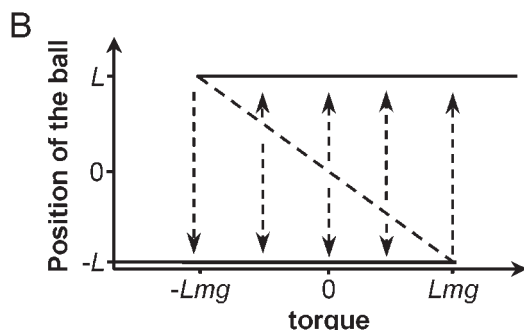


Figure B (Box 1). Bifurcation diagram for the seesaw. We plot the steady-state location of the ball (along the beam) as a function of the applied torque. The solid lines denote stable steady states with the ball at the left stop or the right stop. The dashed line denotes unstable steady states, with the beam horizontal and the ball delicately balanced at some location between the two ends. The (vertical) dashed arrows indicate the direction the ball will move if displaced from the unstable steady state. For values of torque between $-Lmg$ and $+Lmg$, the system is bistable.

counterclockwise force. If we start the experiment with a large positive torque, then clearly the ball will end up at the right stop ($x = L$), which is a stable steady state. As we decrease the torque, the ball stays where it is. Even at small negative torques, the ball stays at the right stop. However, when the torque passes a critical negative value ($\tau_1 = -Lmg$), the seesaw suddenly tips to the other side and the ball ends up at the left stop ($x = -L$). It will stay there, as the torque gets more and more negative. Now let's increase the torque. The ball will stay at the left stop, because it is a stable steady state, until the torque is increased above a critical positive value ($\tau_2 = Lmg$), when the seesaw will tip back to the right-side-down position. The cycle of torque applications that tips the seesaw first to the left and then back to the right is called a hysteresis loop.

Notice that, for intermediate values of torque ($\tau_1 \leq \tau \leq \tau_2$), the dynamical system has two stable steady states ("bistability"). The ball can be at either end of the seesaw, depending on where it started out. Notice that, in the bistable region there exists a third steady state, which is unstable. This steady state is given by $x^* = -\tau/mg$, where x^* is the unstable steady-state position of the ball for some τ between τ_1 and τ_2 . At τ_1 and τ_2 , the unstable steady state coalesces with one or the other stable steady state and the two coalescing states disappear. This is called a "saddle-node" bifurcation. As the parameter τ crosses a bifurcation point (τ_1 or τ_2), the behavioral possibilities of the dynamical system change in a dramatic way, from bistability to monostability. Depending upon the starting location of the ball, it may be forced to roll to the other side as the torque crosses the bifurcation point.

This example illustrates that bistability, unstable steady states, and hysteresis are all interrelated. They derive from positive feedback in the underlying dynamical system. In our example, think of the unstable steady state with the ball at position $x^* < 0$ where its torque exactly balances the torque $\tau > 0$ applied to the end of the beam. If the ball moves a little to the left, its greater moment arm causes the beam to rotate counterclockwise, causing the ball to move further to the left. That's positive feedback.

The cell cycle control system behaves similarly. Figure C shows the bifurcation diagram for the G_2 -part of the control system, based on positive feedback between Cdc2:cyclin and Cdc25 and double-negative feedback between Cdc2:cyclin and Wee1.⁽³⁾ In this case, the "ball" is the activity of Cdc2:cyclin and the "torque" is total cyclin in the cell. A cell with little total cyclin has low Cdc2 activity, because Wee1 is active

and Cdc25 is inactive. By making more cyclin, the cell eventually reaches a bifurcation point, where the interphase steady state (**I**) coalesces with a saddle point and disappears. The cell cycle control system then makes an irreversible transition to a different stable steady state (**M**) with high Cdc2 activity (Wee1 inactive, Cdc25 active). This diagram is the basis of experimental tests of bifurcation theory described in Box 2.

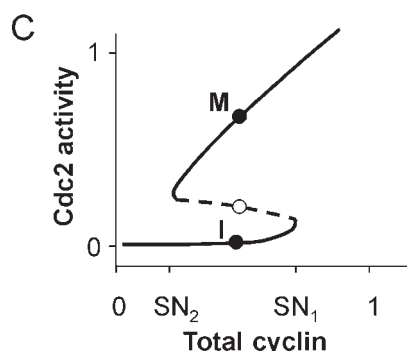


Figure C (Box 1). Bifurcation diagram for the Cdc2–Wee1–Cdc25 module of the cell cycle control system (adapted from Ref. 3). We plot steady state Cdc2 activity as a function of total cyclin in a cell-free extract of frog eggs. For total cyclin concentration between SN_2 and SN_1 (saddle-node bifurcation points), the control system is bistable. The lower stable steady state (● labeled **I** for “interphase”) has low Cdc2 activity, enough to drive DNA synthesis but not mitosis. The upper stable steady state (● labeled **M**) has high Cdc2 activity, sufficient for mitosis. The intermediate steady state (o) is unstable. If enough active Cdc2 is injected into an interphase extract to surmount the unstable steady state, then the extract can be forced into M phase.

Bifurcation diagrams

A primary goal of dynamical systems theory is to characterize the kinds of solutions one can expect to find for a system of nonlinear differential equations (e.g., the kinetic equations that describe a biochemical regulatory network). We are primarily interested in “recurrent” solutions: both steady states (where variables are unchanging in time) and oscillatory states (where variables repeat themselves periodically in time). Recurrent solutions can be either stable or unstable. Stable steady states correspond to conditions of cell cycle arrest, e.g., metaphase arrest induced by drugs that block spindle formation. Stable oscillatory solutions correspond to unmonitored cell divisions, e.g., cell proliferation in early embryos. We will see that normal progress through the cell cycle is subtler than a stable oscillatory solution to the kinetic equations.

The cell cycle control system of fission yeast is characterized by three kinds of steady states and an oscillatory solution. The three steady states are:

- (**G₁**) Very low activity of Cdc2:Cdc13, because Ste9 is actively degrading Cdc13 and Rum1 inhibits any Cdc2:Cdc13 that may appear.
- (**S–G₂**) Intermediate activity of Cdc2:Cdc13, because, although Ste9 and Rum1 are absent, Cdc2:Cdc13 dimers are held in the inactive phosphorylated form, by the action of Wee1 and Mik1.
- (**M**) High activity of Cdc2:Cdc13, because its antagonists (Ste9, Rum1, and Wee1) are all suppressed and its agonist (Cdc25) is active.

The oscillatory solution derives from the negative feedback loop involving Slp1.

Which solution is exhibited by the control system depends on how big the cell is. The relationship between cell size and control-system behavior is summarized in the one-parameter bifurcation diagram in Fig. 3. For the dynamical variable, we choose Cdc2:Cdc13 activity, as representative of the state of the chromosome replication cycle, and for the bifurcation parameter, we choose the mass/nucleus ratio, as representative of the growth cycle of the cell. The diagram keeps track of both steady states and oscillatory states, and distinguishes between stable and unstable solutions.

The complex dynamics of the control system, summarized in the bifurcation diagram, are all implicit in the wiring diagram of the underlying molecular machinery, and they have distinct and clear associations with observable physiological states of the cell cycle (**G₁**, **S–G₂**, and **M** states, with the stable oscillation corresponding to entry into and exit from mitosis).

Very small cells (e.g., cells newly emerged from spores) have only one stable state of the cell cycle control system, namely **G₁**. They must grow to a sufficiently large size (beyond SN_1 in Fig. 3) before they can leave **G₁** phase and enter **S** phase. (In haploid fission yeast cells, this corresponds to a length of approx 5 μm , Ref. 31.) After finishing DNA synthesis, cells remain in the stable **S–G₂** steady state until they reach the critical size (at the SNIC bifurcation in Fig. 3) for entry into mitosis. (In fission yeast, this critical length is approx 11 μm , Ref. 32.) After leaving **G₂** phase, the control system is swept up into the large amplitude, oscillatory state. As Cdc25 removes the inhibitory phosphate group from PCdc2:Cdc13, Cdc2 activity rises sharply, which is the signal for entry into mitosis. Then, as Slp1 promotes degradation of Cdc13, Cdc2 activity falls very low, which is the signal for telophase and cell division. (In fission yeast, division occurs at approx 14 μm , Ref. 33.) The bifurcation parameter, mass/nucleus, drops by a factor of 2, and the control system leaves the domain of existence of the stable oscillatory state.

The new daughter cell is too large (approx 7 μm) to hang around in **G₁** phase. After a brief pause at low Cdc2:Cdc13 activity, as Slp1 activity disappears, the cell proceeds directly into **S–G₂**, and the cell cycle repeats itself. In wild-type cells,

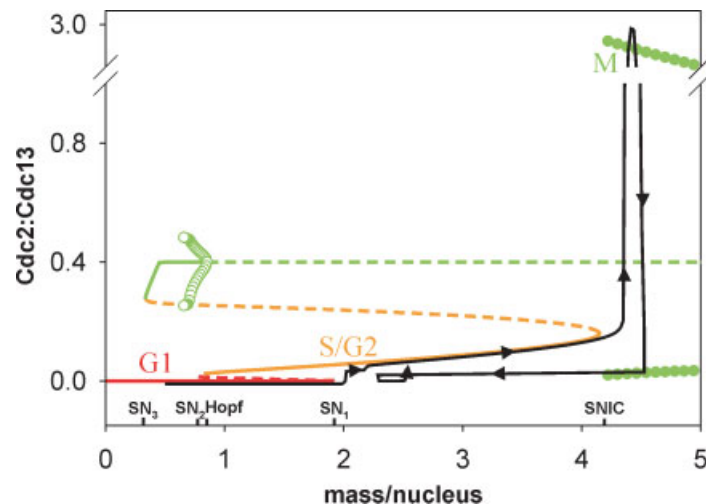


Figure 3. Bifurcation diagram for wild-type cell cycle. Recurrent states of Cdc2:Cdc13 activity are plotted against the mass/nucleus ratio of the cell. At each point along the abscissa, cell mass is held fixed, and the control system is allowed to settle to steady state or oscillatory behavior. For example, at mass/nucleus = 1 (arbitrary unit), the control system has five steady states: two are stable (at [Cdc2:Cdc13] \approx 0 and 0.03), and three are unstable (at [Cdc2:Cdc13] \approx 0.01, 0.3 and 0.4). By increasing and decreasing the mass/nucleus ratio a little bit, the computer can follow the location of these steady states in dependence on the parameter and begin to trace out the five lines on the diagram. Solid lines refer to stable steady states, and dashed lines to unstable steady states. The lines meet at folds, called saddle-node bifurcation points. There are four such points, labeled SN₁, SN₂, SN₃ and SNIC. Unstable oscillatory solutions (open green dots) are found at mass/nucleus \approx 0.8 and stable oscillations (solid green dots) are found at mass/nucleus $>$ 4.15. At a fixed value of mass/nucleus, the upper and lower dots mark the maximum and minimum excursions in Cdc2:Cdc13 activity during an oscillation. See Box 1 for an explanation of steady states, oscillations, stability, and bifurcation. Notice that the locus of steady states is composed of two S-shaped curves as in Figures B and C in Box 1. The lower S curve (solid red, dashed red, solid orange) describes bistability in the G₁–S part of the control system (based on the antagonism between Cdc2:Cdc13 and Rum1 + Ste9). For any mass-to-nucleus ratio between SN₂ and SN₁, there is a stable G₁ state (solid red curve) coexisting with a stable S–G₂ state (solid orange curve), separated by an unstable saddle point (dashed red curve). The saddle-node bifurcation at SN₁ marks the limiting size above which a fission yeast cell must leave G₁ and enter S. The upper S curve (solid orange, dashed orange, green), bounded by saddle-node bifurcations at SN₃ and SNIC, is created by the G₂–M part of the control system (Wee1 and Cdc25). The SNIC bifurcation marks the critical size at which a wild-type fission yeast cell leaves G₂ and enters mitosis. The uppermost steady state (M) is unstable (dashed green) between the Hopf bifurcation on the diagram and a second Hopf bifurcation far off the right side of the diagram. (At a Hopf bifurcation, a steady state loses stability and small amplitude oscillatory solutions arise from the steady state. Oscillations may also bifurcate from a SNIC point—Saddle-Node on an Invariant Cycle, as in the diagram.) In our case, the oscillations are generated by negative feedback in the mitotic exit network (Cdc2:Cdc13 activates Slp1 which then degrades Cdc13). The black line plots the trajectory of a growing cell across the bifurcation diagram, starting from a germinating spore (mass/nucleus = 0.5). For mass/nucleus between 2.2 and 4.4, the black trajectory is derived from the black and green curves in Fig. 2. As the cell grows, the mass/nucleus ratio steadily increases, and the Cdc2:Cdc13 control system adjusts rapidly to find the nearest stable solution of the underlying kinetic equations. Hence, the trajectory seems to cling to stable solutions (solid lines and solid dots) on the bifurcation diagram. But when the mass/nucleus ratio crosses the bifurcation points at SN₁ and SNIC, the control system jumps from one type of stable solution to another, corresponding to a change of phase of the cell cycle. When Cdc2:Cdc13 activity drops below a threshold at the end of mitosis, we assume the cell divides and the mass/nucleus ratio is reset to half its value (from 4.5 to 2.25).

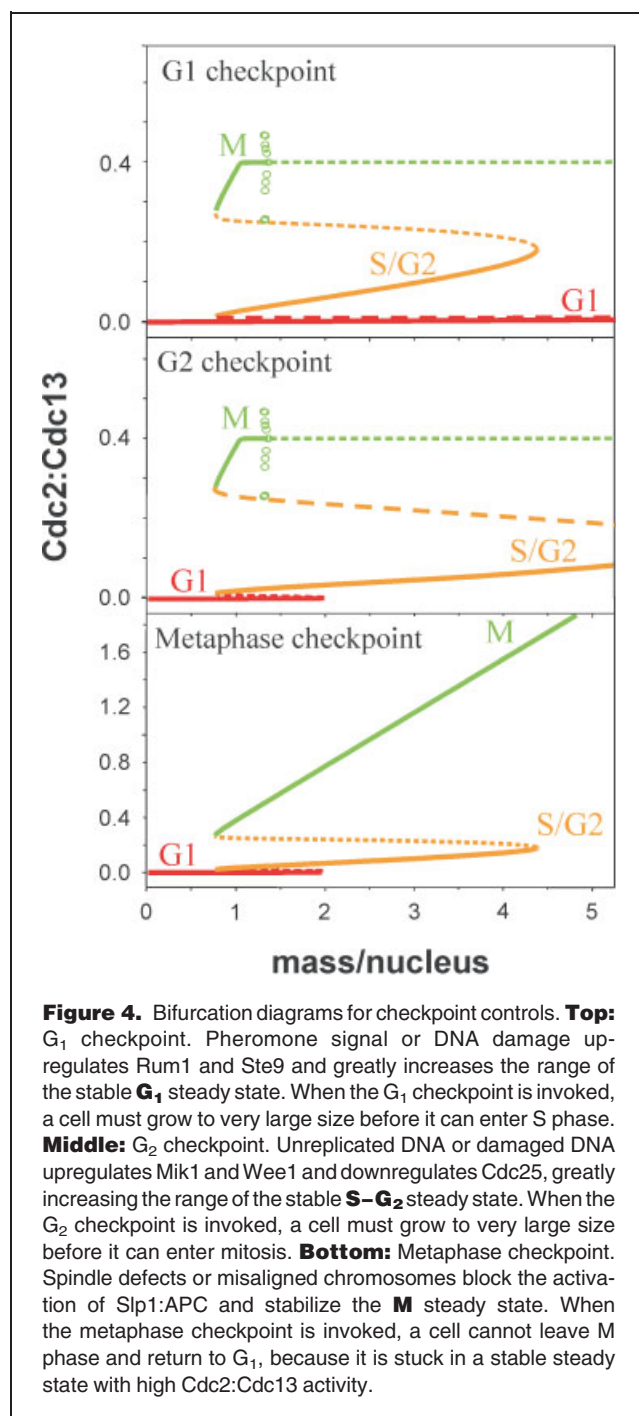
growth and division are coordinated by the critical size requirement at the SNIC bifurcation (the G₂-to-M transition). The size requirement at the G₁-to-S transition (at SN₁) is cryptic in wild-type fission yeast;⁽³⁴⁾ it is only revealed in cells made unusually small by mutation or starvation.

Checkpoints and the Pinocchio effect

In this section, we use bifurcation diagrams (Fig. 4) to explain how checkpoint signals block progress through the cell cycle.

Pheromone

Pheromones are molecules secreted into the extracellular environment to convey to neighboring cells the mating-type identity of the pheromone-secreting cell. When receptor proteins on the surface of a cell of one mating type bind pheromone of a cell of the opposite mating type, the receptors trigger an intracellular signaling pathway that causes the message-receiving cell to halt in G₁ and prepare for mating. From our point of view (Fig. 4, top), the G₁ block induced by mating factor must work



by extending the stable G_1 steady state to large size, i.e., by increasing the critical mass/nucleus ratio for the saddle-node bifurcation that eliminates G_1 .

The “Pinocchio effect” on the nose of the G_1 steady-state curve can be achieved by altering several different parameters, singly or in combination. The obvious candidates are Rum1 and Ste9 (more of them) and starter kinases

(less of them). In fission yeast cells, there is evidence that the pheromone signal works through increasing the amount of Rum1.⁽³⁵⁾

Notice that cells may over-ride pheromone-induced G_1 arrest simply by growing large enough to get around the big nose of the G_1 steady-state curve. This is called adaptation; in fission yeast cells it occurs after about 6 hours.⁽³⁶⁾

Unreplicated or damaged DNA

If, after entering S phase, a cell runs into trouble completing DNA replication, it must delay entry into M phase. A set of proteins that senses unreplicated DNA (persistent replication forks) relays the signal to the cell cycle engine and stabilizes the $S-G_2$ steady state. In fission yeast, unreplicated DNA delays entry into M phase by activating the kinase Mik1 and by inactivating the phosphatase Cdc25.^(37,38) In our picture (Fig. 4, middle), the nose of the $S-G_2$ steady state is extended to large size, and the cell arrests in G_2 .

Notice that this Pinocchio effect must occur transiently even in perfectly normal, wild-type cells: during S phase, when Mik1 is active and Cdc25 is inactive, the $S-G_2$ nose sticks out to very large size, and then retracts into the position indicated in Fig. 3 after DNA replication finishes.

Mutants defective in the replication checkpoint are unable to forestall entry into M phase in the presence of unreplicated DNA. Under normal conditions, this is no problem for the mutant, because DNA replication is completed well before a cell reaches the critical size necessary to enter mitosis (mass/nucleus = 4.15 in Fig. 3). But, in the presence of inhibitors of DNA synthesis, these checkpoint mutants enter mitosis when they reach this critical size, even though their DNA is unreplicated. The unreplicated chromosomes are aligned on the mitotic spindle, but they cannot be separated at anaphase. The undivided nucleus is cut in half by the cell septum, and the mutant cell dies. Since this lethal phenotype manifests itself only in the presence of drugs that inhibit DNA synthesis, it is called a conditional mitotic catastrophe.

Cells also contain DNA-damage surveillance mechanisms that block progress through the cell cycle until radiation-induced damage can be repaired. Damage suffered in G_1 must block entry into S phase by extending the range of stability of the G_1 steady state, whereas damage sustained in S and G_2 phases must block entry into M phase by extending the range of stability of the $S-G_2$ steady state.

We emphasize again that Pinocchio effects can be achieved by variations in many different parameters in the model; hence, one should not be surprised if these checkpoints are implemented by different molecular mechanisms in different organisms.

Spindle assembly and chromosome alignment

If a cell runs into problems assembling its mitotic spindle or aligning all its chromosomes on the spindle, then a spindle

surveillance mechanism delays the metaphase-to-anaphase transition. Because cells exit mitosis by activating Slp1:APC, the mitotic checkpoint works by blocking the activation of these components by Cdc2:Cdc13.⁽¹⁸⁾ Interruption of the negative feedback loop destroys the stable oscillatory state in Fig. 3 and stabilizes the **M** steady state (Fig. 4, bottom). The stable **M** steady state has high Cdc2:Cdc13 activity because Slp1 is completely inactivated when the mitotic checkpoint is engaged.

Mutants

Molecular geneticists deduced the wiring diagram of the cell cycle control system by creating and analyzing mutants defective in cell cycle progression. Most of these mutants are blocked at some stage in the cell division cycle (*cdc* mutants) and are not particularly interesting from a dynamical point of view. But some mutants are viable: they get through all the events of the cell cycle but in some curious way that is noticeably differ-

ent from wild-type cell cycle progression. Though the cell cycle engine continues to turn in these mutants, it turns in a different way, and the defect shows up dramatically in the bifurcation diagram of the mutant control system (Figs. 5 and 6).

Size control

While searching for temperature-sensitive *cdc* mutants in fission yeast in the early 1970s, Paul Nurse discovered an odd mutant, *wee1^{ts}*, which, at the elevated temperature (35°C), grows and divides as rapidly as wild-type cells but is only about half the normal size at division.⁽³⁹⁾ Wild-type cells have short G₁ and long G₂ phases, because they must grow to a large size (Fig. 3) before they may leave S–G₂ and enter mitosis. By contrast, *wee1^{ts}* cells have long G₁ and short G₂ phases, and their size control seems to operate at the G₁-to-S transition.^(34,39) Because Wee1 is nonfunctional in these mutant cells (at 35°C), they lack the large **S–G₂** nose in the bifurcation diagram (Fig. 5, top). The limiting step in progress through the

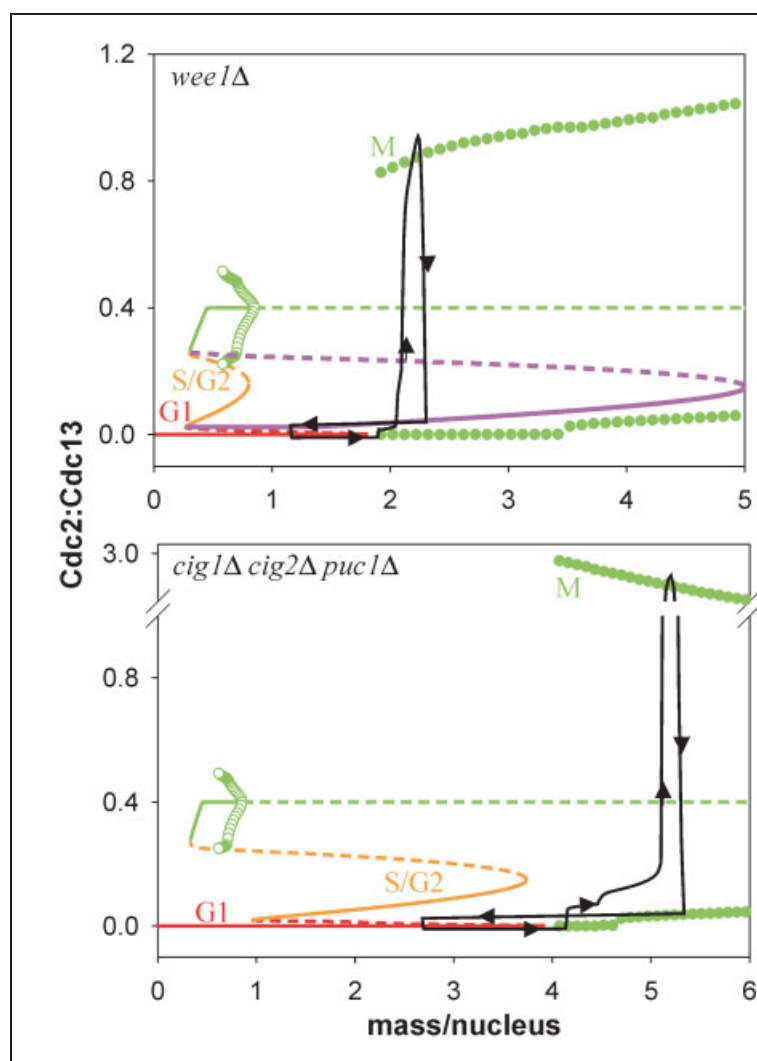


Figure 5. Bifurcation diagrams for size mutants.

Top: *wee1Δ*. Compared to wild-type cells (Fig. 3), the S–G₂ nose (orange) is much reduced because Wee1 is absent. The black curve is a cell cycle trajectory. Let's start with a cell as it exits mitosis at mass/nucleus = 2.3 (about half the size of wild-type cells at division). The newborn daughter (mass/nucleus = 1.15) is attracted to the stable **G₁** state of the control system, and cannot leave this state until it grows to the SNIC bifurcation at mass/nucleus = 1.8. Once past this critical size requirement, the cell enters S phase. While in S phase, Mik1 is active and a temporary S–G₂ nose—the purple curve—is in place. Once S phase is complete, Mik1 turns off and the purple curve retracts to the orange curve. The cell cycle trajectory is immediately captured by the stable limit cycle and the cell enters mitosis after a very brief G₂ phase. Notice that, for the double mutant cell, *wee1^{ts} mik1Δ* at the restrictive temperature, there is no temporary S–G₂ nose. Upon exiting G₁, the cell goes directly into mitosis before it can replicate its DNA. This is a lethal mitotic catastrophe. **Bottom:** *cig1Δ cig2Δ puc1Δ*. Compared to wild-type cells, the G₁ nose (red) is greatly extended. A newborn cell cannot leave G₁ until it grows to mass/nucleus = 3.96. After a brief pause for S phase, as before, the cell proceeds directly into mitosis (black curve). The mutant phenotype is long G₁ phase, short G₂, large size at division, compared to wild-type, exactly as later observed.⁽⁴²⁾

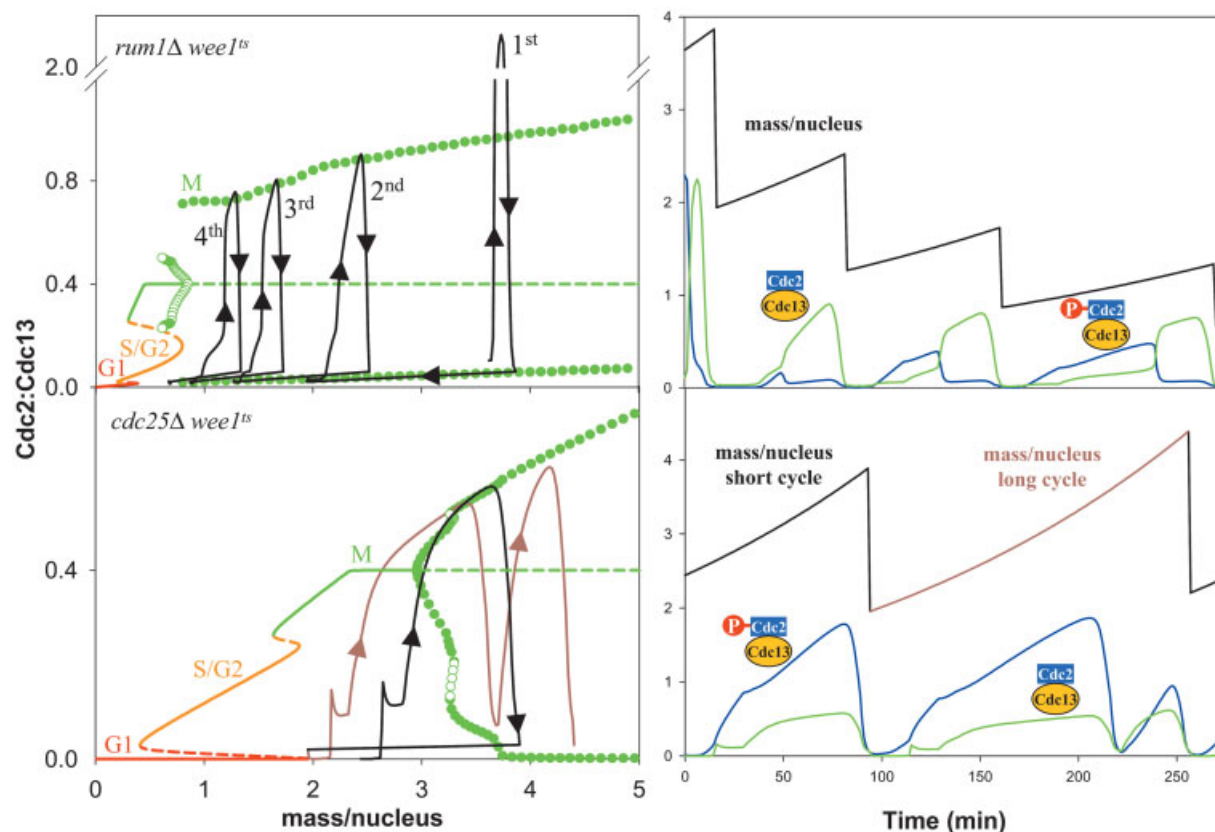


Figure 6. Dynamically challenged mutants. Bifurcation diagrams on the left, numerical simulations on the right. **Top:** *wee1^{ts} rum1Δ*. All bifurcations have been pushed to small size. At the permissive temperature, the cell is viable and only slightly smaller than wild-type. When shifted to the restrictive temperature, the cell divides rapidly and gets progressively smaller (1st, 2nd, 3rd, 4th divisions on the black trajectory) until it dies. **Bottom:** *wee1^{ts} cdc25Δ*. The mitotic steady state (**M**) is stable at first, then loses stability by a Hopf bifurcation at mass/nucleus = 2.95. Small amplitude oscillations (solid green dots) around the unstable **M** state may cause difficulties in exit from mitosis. The first cycle (black trajectory) is quite normal, but the second cycle (brown trajectory) is abnormal. The cell's first attempt to exit mitosis is aborted because Cdc2:Cdc13 activity does not drop low enough for telophase to occur. On its second try, the cell successfully rids itself of Cdc13 and can divide. A population of such cells will exhibit a bimodal distribution of cycle times with peaks at 94 minutes and 164 minutes, which is intriguingly close to the observed behavior of these mutants.⁽⁴⁶⁾

cell cycle appears to be growing large enough to pass the SNIC bifurcation point where the **G₁** steady state is lost.

This explanation, though basically correct, is incomplete. *wee1^{ts}* cells still contain functional Mik1 and Cdc25. Unreplicated DNA activates Mik1 and inhibits Cdc25, so Cdc2 becomes tyrosine-phosphorylated even in the absence of Wee1. On the bifurcation diagram, when cells surpass the **G₁** nose and enter S phase, there is a temporary appearance of a large **S–G₂** nose, because the unreplicated-DNA checkpoint is still intact. As soon as DNA replication is complete, this nose disappears, and there is nothing to prevent *wee1^{ts}* cells from entering mitosis immediately. Hence, they have a short G₂ phase, but they respond perfectly normally to inhibitors of DNA synthesis.

When *wee1^{ts} mik1Δ* double-mutant cells are shifted to the restrictive temperature, the rise in Cdc2:Cdc13 activity after

the G₁-to-S transition is not blocked because, although Cdc25 is down-regulated, there are no tyrosine kinases to inactivate Cdc2. Hence, there is no temporary Pinocchio effect, so these double-mutant cells enter directly into mitosis before they can finish the job of DNA synthesis, with fatal results.⁽²⁴⁾ This is an unconditional mitotic catastrophe because it happens even if DNA replication is not blocked by drugs or mutations.⁽⁴⁰⁾ Similarly, *wee1^{ts} hus1Δ* double-mutant cells also suffer mitotic catastrophe at the restrictive temperature,⁽⁴¹⁾ because, lacking Hus1, they cannot relay the temporary Pinocchio signal to Mik1.

While Wee1 determines cell size at the G₂-to-M transition, the starter kinases determine size at the G₁-to-S transition.⁽⁴²⁾ When the three G₁ cyclins are deleted (*cig1Δ cig2Δ puc1Δ*), cells must reach a much larger size to surpass the **G₁** nose (Fig. 5, bottom). As soon as they are finished DNA synthesis

(that checkpoint is still intact), they will enter mitosis immediately, because the G_2 size requirement is already satisfied. Hence, these triple-mutant cells have long G_1 and short G_2 phases, like *wee1^{ts}*, but they are larger than normal rather than smaller. Extension of the G_1 nose in *cig1 Δ cig2 Δ puc1 Δ* is dependent on Rum1 and disappears completely in a quadruple mutant cell, *cig1 Δ cig2 Δ puc1 Δ rum1 Δ* , whose phenotype is identical to a wild-type cell.⁽⁴²⁾

Complex dynamics

The mutants described in Fig. 5 demonstrate the crucial role played by Wee1 in stabilizing the **S– G_2** state. In the absence of Wee1, cells enter prematurely into M phase. Similarly, Rum1 plays a crucial role in stabilizing the **G_1** state. In the absence of Rum1, cells cycle just like wild type, with short G_1 phase, but they cannot stop in G_1 .^(22,43) For example, pheromone cannot induce G_1 arrest in *rum1 Δ* cells,⁽³⁵⁾ and hence they are sterile. When both Wee1 and Rum1 are missing (in *wee1^{ts} rum1 Δ* double mutants), both G_1 and G_2 control modules are compromised,⁽⁴⁴⁾ and the oscillatory character of the mitotic module is revealed (Fig. 6, top). The double mutant is inviable. At 25°C, when Wee1 is active, the cells are perfectly normal. When shifted to 35°C, to inactivate the mutant Wee1 protein, the double-mutant cells undergo a series of rapid mitotic cycles, getting smaller and smaller each cycle until they perish.⁽²²⁾ Clearly, the period of the oscillator is shorter than the mass doubling time, and this is a fatal mistake. In principle, cell size should eventually fall below the SNIC bifurcation point (Fig. 6, top) and size control should be reasserted, but apparently such small size is incompatible with viability of fission yeast.

Wee1 is an inhibitor for mitosis and Cdc25 is an activator. The simple prediction that the activator is not needed in the absence of the inhibitor is partially born out, since *wee1^{ts} cdc25 Δ* double mutants are viable.⁽⁴⁵⁾ However, these cells are larger than wild-type cells on average, and their length at division is very variable. Moreover, the distribution of interdivision times in an asynchronous culture of *wee1^{ts} cdc25 Δ* cells is multimodal, with peaks of decreasing magnitudes at 100 minutes, 170 minutes, and 240 minutes.⁽³³⁾ The bifurcation diagram for *wee1^{ts} cdc25 Δ* (Fig. 6, bottom) gives some insight into this curious phenotype.⁽³⁰⁾ The Hopf bifurcation creating the mitotic oscillator now occurs at mass/nucleus ratio above the saddle-node bifurcations. Because the oscillations arising from the Hopf bifurcation have small amplitude initially, they do not drive robust progression through mitosis (exit from mitosis seems to require reduction of Cdc2:Cdc13 activity to very low level). The simulations (Fig. 6, bottom) show two types of cell cycles. A large newborn cell (mass/nucleus = 2.2) progresses normally through mitosis and has a short interdivision time, but a small newborn cell (mass/nucleus = 1.95) is unable to exit mitosis on the first pass, tries again with success, and consequently has a long interdivision time. By

superimposing some molecular noise on this deterministic model, it is possible to simulate quite faithfully the distributions of size and cycle time in these mutant cells.⁽⁴⁶⁾

Conclusions

The physiological characteristics of a cell are determined by networks of interacting proteins that process energy, material and information. Confined to a few picoliters of cytoplasm, these processing and control systems are not only as complex as a Boeing 777 but are also able to make exact replicas of themselves from CO_2 , NO_3^- , PO_4^{3-} , and a drop of mineral water. We would like to know how these marvelous machines work, but they do not come with instruction manuals or schematic wiring diagrams. It is the grand challenge for post-genomic life scientists to deduce the diagrams and write the manuals. This effort will take a variety of resources and approaches: genetics and biochemistry, hardware and software, high-throughput and low-throughput technologies, hypothesis-driven and discovery-driven experiments, silicon-based and myelin-based reasoning.

Our contribution to this enterprise is a careful analysis of the kinetic properties of small regulatory networks (10–50 differential equations). We use computer simulation to compare model behavior to experimental observations, and bifurcation theory to uncover the dynamical principles of control systems. In Box 2, we summarize how mathematical modeling complements the reductionist approach of biochemists and molecular geneticists, and we describe some recent experimental confirmations of basic predictions of the models.

In this review, we have tried to show that one-parameter bifurcation diagrams give a new and useful perspective on the growth and reproduction of fission yeast. From this perspective, progress through the cell division cycle is a sequence of bifurcations between stable recurrent states of the three subsystems of the regulatory network: the G_1 , S– G_2 , and mitotic modules. Passing these bifurcation points is driven by cell growth (mass/nucleus ratio), and progress from one stage of the cycle to the next can be restrained by checkpoint mechanisms that monitor the state of the cell's DNA and mitotic apparatus. If there are problems, these checkpoint mechanisms push the bifurcation points to larger size and thereby halt (or delay) progression through the cell cycle.

Much of what biologists know about the molecular machinery regulating the cell cycle was deduced from the phenotypes of cell cycle mutants of budding yeast and fission yeast. Some of these mutants have very strange properties: small size, mitotic catastrophes, quantized cycles, and suicide by repeated divisions. Mutations change protein activities, which modify kinetic parameters in the model, which distort the bifurcation diagram of the control system, which reorganizes progression through the cell cycle. By seeing how mutations change bifurcation diagrams, we get an insider's view of how phenotype is determined by genotype.

BOX 2: WHAT IS THE “VALUE-ADDED” BY MATHEMATICAL MODELING?

What does the model teach us that we don't already know?

Over the past 20 years, molecular cell biologists have been very successful in identifying the genes and protein interactions that underlie progression through the eukaryotic cell cycle, culminating in the award of Nobel prizes to Hartwell, Hunt and Nurse in 2001. These bits and pieces of the cell cycle “puzzle” can be assembled into attractive cartoons (box-and-arrow diagrams) that are remarkably useful in organizing information and suggesting new experiments. But how much do these cartoons really tell us? Do they provide a satisfying, reliable, consistent, believable picture of cell cycle control?

As currently interpreted, BioCarta-type cartoons certainly do not provide a quantitative account of all the experimental data they are supposed to summarize. They are used only in a loose, qualitative fashion, to frame informal, verbal explanations of observations. Hand-waving arguments may be sufficient for designing new experiments; after all, experimental results speak for themselves, regardless of the reasons for which they were conducted. But they are not reliable for judging the verity of mechanistic proposals. How can we tell whether our diagrams and verbal explanations are faithful representations of reality or more like a Bugs Bunny cartoon—witty and entertaining, but internally inconsistent and ultimately in deep contradiction to reality? Perhaps we know less than we think we know. Perhaps we are seduced by the cartoon's appeal into thinking that we understand what is still a mystery.

For instance, why does a fertilized frog egg undergo a sequence of 12 rapid, synchronous mitotic cycles before the MBT? “Because cyclin is alternately synthesized and degraded in each cycle,” we are told. Why? “Because the cyclin-degradation machinery is activated by high levels of Cdc2:cyclin.” Why doesn't the system come to a stable steady state, where the rate of synthesis of cyclin is exactly balanced by its rate of degradation? “Why should it?” Well, that's the case for most proteins. What's so special about cyclins? “Cyclins are special by definition. They are periodically degraded. Quit pestering me with your theoretical hang-ups.” Well, it is not particularly easy to get a molecular reaction network to oscillate. Very specific conditions must be satisfied. Is there any evidence that these conditions are met in the early frog embryo? What's different about the unfertilized frog egg, where the same

network is blocked in a stable steady state? “The unfertilized egg is full of CSF.” What does CSF do? “It blocks the egg in meiotic metaphase.” And so the conversation goes, the outsider wanting to know why, and the insider appealing ultimately to the very observations that he or she claims to understand.

There is a scientific way to test the reliability and consistency of our informal ideas about molecular regulation. We must cast our hypotheses (cartoons) in precise mathematical terms, compute accurate solutions of the equations, and compare the solutions in quantitative detail with a wide variety of experimental observations. It is no mean feat to carry out this test, and it tells us something that we definitely did not know beforehand: whether or not our model is an accurate representation of reality. In most cases, we find that our first reasonable guess about the wiring diagram is insufficient to account for a number of central experimental facts. The initial hypothesis needs to be revised and refined until (if we understand the control system well enough) the mathematical model can be brought into accord with all the basic facts.

What predictions does the model make? Are they born out by experiment?

If our models are indeed accurate, then they should make reliable predictions. We might also expect the models to provide new insights into cell cycle regulation and to suggest experiments that were unanticipated beforehand.

The most fundamental ideas behind our model of cell cycle controls are the notions of bistability, hysteresis, and bifurcation. These ideas were presented in a 1993-paper,⁽³⁾ where Fig. C (Box 1) first appeared. If this bifurcation diagram is true, then the G₂-control system should be bistable for intermediate levels of cyclin. The prediction is easily tested in frog egg extracts, where total cyclin concentration can be controlled experimentally. Indeed, Solomon et al.⁽⁵⁴⁾ had already done the first part of the test in 1990. They demonstrated the existence of a distinct cyclin threshold for Cdc2 activation (namely SN₁) in Fig. C. But only recently has the existence of the second threshold (SN₂ in Fig. C, for Cdc2 inactivation) been demonstrated experimentally, by three different groups (Jonathon Moore, Pomerening & Ferrell, Sha & Sible, private communications).

Novak and Tyson⁽³⁾ made two other predictions. For cyclin concentrations slightly larger than SN₁, the time lag for MPF activation should become very long. In dynamical systems theory, this is a generic effect close to saddle-node bifurcations, called “critical slowing down.” Secondly, in the presence of unreplicated

DNA, the cyclin threshold for Cdc2 activation should be greatly increased (the “Pinocchio effect”). Moore, Sha & Sible have verified both of these predictions as well (unpublished).

Bistability and hysteresis play major roles in yeast cell cycle control as well. Chen et al.⁽²⁾ made specific suggestions about how to test for bistability in budding yeast. The predictions were confirmed recently by Cross et al.⁽⁵⁵⁾ who showed that, under identical conditions, yeast cells can arrest either in G₁ phase or in S–G₂ phase, depending on how the cells are prepared. Cross and colleagues have reported other tests of Chen’s model, including size dependence on cyclin gene dosage and cyclin localization to the nucleus,⁽⁵⁶⁾ and the absolute and relative abundances of regulatory proteins in wild-type and mutant cells.

The yeast models can also be used to predict phenotypes of mutants that have not yet been constructed. For instance, the phenotype of the starter kinase-deletion mutant in Fig. 5 was predicted in 1998⁽⁵⁷⁾ and confirmed in 2000.⁽⁴²⁾ By a similar interplay of simulation and experiment, Cross and Chen have been studying exit from mitosis in budding yeast by novel combinations of mutations in the genes encoding APC, Cdc20, Cdc14, Cdh1, Sic1, and Cdc6 (homologs of Slp1, Ste9, Rum1, etc., in fission yeast). The model predicted correctly the phenotypes of the following mutants: *APC-A* (non-phosphorylatable form of APC, viable), *APC-A cdh1* (inviable), *APC-A cdh1GAL-SIC1* (viable), *APC-A cdh1 GAL-CDC20* (viable) (Cross, private communication).

Lastly, the model can be used to estimate (predict) the values of kinetic rate constants that are difficult to measure directly. This fact is counterintuitive. Many people argue that a model with so many free parameters must easily be fit to experiments by many different sets of parameter values, and that the parameter values therefore are biochemically meaningless. The opposite is apparently true. Kinetic constants in the 1993 frog-egg model⁽³⁾ were chosen to fit the model to a broad spectrum of qualitative facts about the frog egg cell cycle. In 1994–95, two experimental papers appeared,^(58,59) reporting careful measurements of the rates of phosphorylation and dephosphorylation of Cdc2, Cdc25 and Wee1 in frog egg extracts in interphase and in M phase. From these data one can estimate directly the rate constants for these crucial steps in the model,⁽⁶⁰⁾ and the values come out very close to the original estimates of Novak and Tyson.⁽³⁾

We believe this approach holds great promise for tracing the connections from genes to networks to behaviors.

Acknowledgments

For refining our ideas on cell cycle regulation, we are grateful for conversations with colleagues and collaborators: Paul Nurse, Jacky Hayles, Kim Nasmyth, Fred Cross, Jill Sible, Kathy Chen, Bela Györfy, and Akos Sveiczler.

References

- Hartwell LH, Hopfield JJ, Leibler S, Murray AW. From molecular to modular cell biology. *Nature* 1999;402:C47–C52.
- Chen KC, Csikasz-Nagy A, Györfy B, Val J, Novak B, Tyson JJ. Kinetic analysis of a molecular model of the budding yeast cell cycle. *Mol Biol Cell* 2000;11:369–391.
- Novak B, Tyson JJ. Numerical analysis of a comprehensive model of M-phase control in *Xenopus* oocyte extracts and intact embryos. *J Cell Sci* 1993;106:1153–1168.
- Novak B, Tyson JJ. Modeling the control of DNA replication in fission yeast. *Proc Natl Acad Sci USA* 1997;94:9147–9152.
- Novak B, Csikasz-Nagy A, Györfy B, Nasmyth K, Tyson JJ. Model scenarios for evolution of the eukaryotic cell cycle. *Philos Trans R Soc Lond B Biol Sci* 1998;353:2063–2076.
- Tyson JJ, Novak B. Regulation of the eukaryotic cell cycle: molecular antagonism, hysteresis, and irreversible transitions. *J Theor Biol* 2001;210:249–263.
- Tyson JJ, Novak B, Odell GM, Chen K, Thron CD. Chemical kinetic theory: understanding cell-cycle regulation. *Trends Biochem Sci* 1996;21:89–96.
- Nasmyth K, Peters JM, Uhlmann F. Splitting the chromosome: cutting the ties that bind sister chromatids. *Science* 2000;288:1379–1385.
- Elledge SJ. Cell cycle checkpoints: preventing an identity crisis. *Science* 1996;274:1664–1672.
- Gardner RD, Burke DJ. The spindle checkpoint: two transitions, two pathways. *Trends Cell Biol* 2000;10:154–158.
- Lew DJ. Cell-cycle checkpoints that ensure coordination between nuclear and cytoplasmic events in *Saccharomyces cerevisiae*. *Curr Opin Genet Dev* 2000;10:47–53.
- Le Goff X, Woollard A, Simanis V. Analysis of the *cps1* gene provides evidence for a septation checkpoint in *Schizosaccharomyces pombe*. *Mol Gen Genet* 1999;262:163–172.
- Cerutti L, Simanis V. Controlling the end of the cell cycle. *Curr Opin Genet Dev* 2000;10:65–69.
- Zachariae W, Nasmyth K. Whose end is destruction: cell division and the anaphase-promoting complex. *Genes Dev* 1999;13:2039–2058.
- Stern B, Nurse P. A quantitative model for the cdc2 control of S phase and mitosis in fission yeast. *Trends Genet* 1996;12:345–350.
- Fisher D, Nurse P. Cyclins of the fission yeast *Schizosaccharomyces pombe*. *Semin Cell Biol* 1995;6:73–78.
- Blanco MA, Sanchez-Diaz A, de Prada JM, Moreno S. APC(ste9/srw1) promotes degradation of mitotic cyclins in G(1) and is inhibited by cdc2 phosphorylation. *EMBO J* 2000;19:3945–3955.
- Kim SH, Lin DP, Matsumoto S, Kitazono A, Matsumoto T. Fission yeast Slp1: an effector of the Mad2-dependent spindle checkpoint. *Science* 1998;279:1045–1047.
- Kitamura K, Maekawa H, Shimoda C. Fission yeast Ste9, a homolog of Hct1/Cdh1 and Fizzy-related, is a novel negative regulator of cell cycle progression during G₁-phase. *Mol Biol Cell* 1998;9:1065–1080.
- Yamaguchi S, Murakami H, Okayama H. A WD repeat protein controls the cell cycle and differentiation by negatively regulating Cdc2/B-type cyclin complexes. *Mol Biol Cell* 1997;8:2475–2486.
- Correa-Bordes J, Nurse P. p25^{rum1} orders S phase and mitosis by acting as an inhibitor of the p34^{cdc2} mitotic kinase. *Cell* 1995;83:1001–1009.
- Moreno S, Nurse P. Regulation of progression through the G₁ phase of the cell cycle by the rum1⁺ gene. *Nature* 1994;367:236–242.

23. Yamaguchi S, Okayama H, Nurse P. Fission yeast Fizzy-related protein *sw1p* is a G(1)-specific promoter of mitotic cyclin B degradation. *EMBO J* 2000;19:3968–3977.
24. Lundgren K, Walworth N, Booher R, Dembski M, Kirschner M, Beach D. *mik1* and *wee1* cooperate in the inhibitory tyrosine phosphorylation of *cdc2*. *Cell* 1991;64:1111–1122.
25. Millar JB, Russell P. The *cdc25* M-phase inducer: an unconventional protein phosphatase. *Cell* 1992;68:407–410.
26. Hanahan D, Weinberg RA. The hallmarks of cancer. *Cell* 2000;100:57–70.
27. Tyson JJ, Chen KC, Novak B. Network dynamics and cell physiology. *Nature Rev Mol Cell Biol* 2002;2:908–916.
28. Russell P, Nurse P. Negative regulation of mitosis by *wee1*⁺, a gene encoding a protein kinase homolog. *Cell* 1987;49:559–567.
29. Russell P, Nurse P. *cdc25*⁺ functions as an inducer in the mitotic control of fission yeast. *Cell* 1986;45:145–153.
30. Novak B, Pataki Z, Ciliberto A, Tyson JJ. Mathematical model of the cell division cycle of fission yeast. *Chaos* 2001;11:277–286.
31. Nurse P, Thuriaux P. Controls over the timing of DNA replication during the cell cycle of fission yeast. *Exp Cell Res* 1977;107:365–375.
32. Creanor J, Mitchison JM. The kinetics of H1 histone kinase activation during the cell cycle of wild-type and *wee* mutants of the fission yeast *Schizosaccharomyces pombe*. *J Cell Sci* 1994;107(Pt 5):1197–1204.
33. Sveiczzer A, Novak B, Mitchison JM. The size control of fission yeast revisited. *J Cell Sci* 1996;109:2947–2957.
34. Fantes PA, Nurse P. Control of the timing of cell division in fission yeast. Cell size mutants reveal a second control pathway. *Exp Cell Res* 1978;115:317–329.
35. Stern B, Nurse P. Cyclin B proteolysis and the cyclin-dependent kinase inhibitor *rum1p* are required for pheromone-induced G₁ arrest in fission yeast. *Mol Biol Cell* 1998;9:1309–1321.
36. Stern B, Nurse P. Fission yeast pheromone blocks S-phase by inhibiting the G₁ cyclin B-p34^{cdc2} kinase. *EMBO J* 1997;16:534–544.
37. Rhind N, Russell P. Roles of the mitotic inhibitors *Wee1* and *Mik1* in the G(2) DNA damage and replication checkpoints. *Mol Cell Biol* 2001;21:1499–1508.
38. Furnari B, Blasina A, Boddy MN, McGowan CH, Russell P. *Cdc25* inhibited in vivo and in vitro by checkpoint kinases *Cds1* and *Chk1*. *Mol Biol Cell* 1999;10:833–845.
39. Nurse P. Genetic control of cell size at cell division in yeast. *Nature* 1975;256:547–551.
40. Novák B, Tyson JJ. Quantitative analysis of a molecular model of mitotic control in fission yeast. *J Theor Biol* 1995;173:283–305.
41. Enoch T, Carr AM, Nurse P. Fission yeast genes involved in coupling mitosis to completion of DNA replication. *Genes Dev* 1992;6:2035–2046.
42. Martin-Castellanos C, Blanco MA, de Prada JM, Moreno S. The *puc1* cyclin regulates the G₁ phase of the fission yeast cell cycle in response to cell size. *Mol Biol Cell* 2000;11:543–554.
43. Kominami K, Seth-Smith H, Toda T. *Apc10* and *Ste9/Srw1*, two regulators of the APC-cyclosome, as well as the CDK inhibitor *Rum1* are required for G₁ cell-cycle arrest in fission yeast. *EMBO J* 1998;17:5388–5399.
44. Moreno S, Labib K, Correa J, Nurse P. Regulation of the cell cycle timing of Start in fission yeast by the *rum1*⁺ gene. *J Cell Sci Suppl* 1994;18:63–68.
45. Enoch T, Gould KL, Nurse P. Mitotic checkpoint control in fission yeast. *Cold Spring Harb Symp Quant Biol* 1991;56:409–416.
46. Sveiczzer A, Tyson J, Novak B. A stochastic, molecular model of the fission yeast cell cycle: role of the nucleocytoplasmic ratio in cycle time regulation. *Biophys Chem* 2001;92:1–15.
47. Tyson JJ, Mackey MC, editors. Focus Issue: Molecular, metabolic, and genetic control. *Chaos* 2001;11:81–292.
48. Hasty J, McMillen D, Isaacs F, Collins JJ. Computational studies of gene regulatory networks: in numero molecular biology. *Nat Rev Genet* 2001;2:268–279.
49. Smolen P, Baxter DA, Byrne JH. Mathematical modeling of gene networks. *Neuron* 2000;26:567–580.
50. Edelstein-Keshet L. *Mathematical Models In Biology*. New York: McGraw Hill Text. 1988.
51. Fall C, Marland E, Wagner J, Tyson JJ. *Computational Cell Biology*. New York: Springer Verlag. 2002.
52. Kaplan D, Glass L. *Understanding Nonlinear Dynamics*. New York: Springer Verlag. 1997.
53. Strogatz SH. *Nonlinear Dynamics and Chaos: With Applications to Physics, Biology, Chemistry and Engineering*. Cambridge, MA: Perseus Books. 1994.
54. Solomon MJ, Glotzer M, Lee TH, Philippe M, Kirschner MW. Cyclin activation of p34^{cdc2}. *Cell* 1990;63:1013–1024.
55. Cross FR, Archambault V, Miller M, Klovstad M. Testing a mathematical model of the yeast cell cycle. *Mol Biol Cell* 2002;13:52–70.
56. Miller ME, Cross FR. Mechanisms controlling subcellular localization of the G(1) cyclins *Cln2p* and *Cln3p* in budding yeast. *Mol Cell Biol* 2001;21:6292–6311.
57. Novak B, Csikasz-Nagy A, Gyorffy B, Chen K, Tyson JJ. Mathematical model of the fission yeast cell cycle with checkpoint controls at the G₁/S, G₂/M and metaphase/anaphase transitions. *Biophys Chem* 1998;72:185–200.
58. Kumagai A, Dunphy WG. Control of the *Cdc2*/cyclin B complex in *Xenopus* egg extracts arrested at a G₂/M checkpoint with DNA synthesis inhibitors. *Mol Biol Cell* 1995;6:199–213.
59. Lee TH, Turk C, Kirschner MW. Inhibition of *cdc2* activation by *INH/PP2A*. *Mol Biol Cell* 1994;5:323–338.
60. Marlovits G, Tyson CJ, Novak B, Tyson JJ. Modeling M-phase control in *Xenopus* oocyte extracts: the surveillance mechanism for unreplicated DNA. *Biophys Chem* 1998;72:169–184.